JOC Article

Laser Flash Photolysis and CIDNP Studies of Steric Effects on Coupling Rate Constants of Imidazolidine Nitroxide with Carbon-Centered Radicals, Methyl Isobutyrate-2-yl and *tert*-Butyl Propionate-2-yl[⊥]

Dmitry Zubenko,[†] Yuri Tsentalovich,[†] Nataly Lebedeva,[†] Igor Kirilyuk,[‡]
Galina Roshchupkina,[‡] Irina Zhurko,[‡] Vladimir Reznikov,[‡] Sylvain R. A. Marque,[§] and
Elena Bagryanskaya*,[†]

International Tomography Center SB RAS, Novosibirsk, Russia, Institute of Organic Chemistry SB RAS, Novosibirsk, Russia, and Université de Provence case 542, Avenue Escadrille Normandie-Niemen13397, Marseille Cedex 20, France

elena@tomo.nsc.ru

Received April 13, 2006

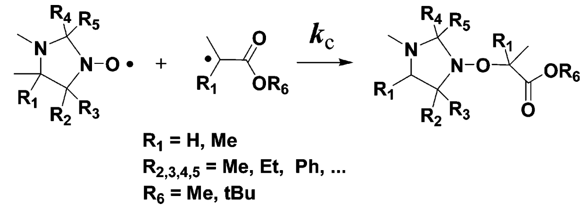

Time-resolved chemically induced dynamic nuclear polarization (TR-CIDNP) and laser flash photolysis (LFP) techniques have been used to measure rate constants for coupling between acrylate-type radicals and a series of newly synthesized stable imidazolidine *N*-oxyl radicals. The carbon-centered radicals under investigation were generated by photolysis of their corresponding ketone precursors RC(O)R (R = $C(CH_3)_2-C(O)OCH_3$ and $CH(CH_3)-C(O)-OtBu$) in the presence of stable nitroxides. The coupling rate constants k_c for modeling studies of nitroxide-mediated polymerization (NMP) experiments were determined, and the influence of steric and electronic factors on k_c values was addressed by using a Hammett linear free energy relationship. The systematic changes in k_c due to the varied steric ($E_{s,n}$) and electronic ($\sigma_{L,n}$) characters of the substituents are well-described by the biparameter equation $\log(k_c/\mathrm{M}^{-1}\mathrm{s}^{-1}) = 3.52\sigma_{L,n} + 0.47E_{s,n} + 10.62$. Hence, k_c decreases with the increasing steric demand and increases with the increasing electron-withdrawing character of the substituents on the nitroxide.

Introduction

Chemical reactions with participation of stable nitroxides have attracted great attention of scientists during the past decades. Nitroxides are widely used as spin labels in biology[1] and as pH probes in biological systems,[2] as mediators in nitroxide mediated polymerization (NMP) due to their possibility of acting as reversible traps for other free-radical species,[3] etc. Recently, the synthesis of a series of imidazolidine nitroxides has been reported which have different bulky substituents at positions 2 and 5 of the imidazolidine ring (**1**−**4** in Table 1).[4] It was shown that they can be successfully applied as pH sensitive spin probes in biological systems.[5] The most important finding was the fact that these new nitroxides were 20−30 times more stable in the presence of ascorbate and had significantly longer half-lives in rat blood as compared to 2,2,5,5-tetra-Me analogues. But the

---

[*] Address correspondence to this author.

[⊥] In memory of Hanns Fischer.

[†] International Tomography Center.

[‡] Institute of Organic Chemistry SB RAS.

[§] Université de Provence case 542.

(1) Volodarskii, L. B. *Imidazoline Nitroxides*; CRC Press: Boca Raton, FL, 1988. Kocherginsky, N.; Swarts, H. M. *Nitroxide Spin Labels*; *Reactions in Biology and Chemistry*; CRC Press: Boca Raton, FL, 1995.

(2) Khramtsov, V. V.; Grigor'ev, I. A.; Foster, M. A.; Lurie, D. J.; Nicholson, I. *Cell. Mol. Biol.* (*Paris*) **2000**, *46*, 1361−1374.

(3) Solomon, D. H. *J. Polym. Sci. Part A*: *Polym. Chem.* **2005**, *43*, 5748−5764.

(4) Kirilyuk, I. A.; Bobko, A. A.; Grigor'ev, I. A.; Khramtsov, V. V. *Org. Biomol. Chem.* **2004**, *2*, 1025−1030.

(5) Bobko, A. A.; Khramtsov, V. V.; Grigor'ev, I. A. *Org. Biomol. Chem.* **2005**, *3*, 1269−1274.

10.1021/jo060787x CCC: $33.50

TABLE 1. Recombination Rate Constants k_c for Nitroxides 1−4, 8a−g, and 12 and Radicals MiB and TBP at Room Temperature, with Their Electrical Hammett Constants $\sigma_{L,n}$ and Steric Constants $E_{s,n}$

Nitroxides		k_c (tBP)[a] 10^{-8}M s	k_c (MiB)[a] 10^{-8}M s	σ_L[b,c]	$E_{s,n}$[d,e]	$E_{s,n}$[d,f]	a_N[g]
1	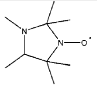	6.3 ±0.8[h]	7.8 ±1.9[h]	0.12	–4.20	–4.20	1.44
2	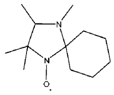	3.8 ±1.4	3.4 ±1.2	0.12	–6.26[i]	–5.21[i]	1.43
3	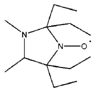	1.6±0.4	1.2±0.4	0.12	–8.32	–6.20	1.35
4	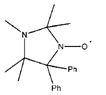	–[j]	1.4±0.4	0.38	–11.78[i]	–7.89	-[j]
8a	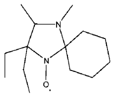	–[j]	0.64±0.18[h]	0.12	–8.32[i]	–6.20[i]	1.38
8b	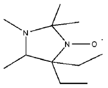	–[j]	3.4±0.4	0.12	–6.26	–5.21	-[j]
8c	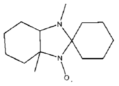	–[j]	2.8 ±0.8	0.12	–7.01[i]	–5.21[i]	1.46
8d	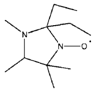	2.6±0.7	3.4±0.7	0.12	–6.26	–5.21	1.37
8e	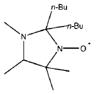	2.9±0.4	2.8±0.7	0.12	–6.26[i]	–5.21[i]	1.39
8f	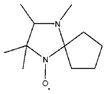	7.0±1.5	8.6±0.5	0.12	–4.20[i]	–4.20[i]	1.43
8g	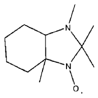	6.2±1.3	8.2 ±1.2	0.12	–4.96[i]	–4.45[i]	1.43
12	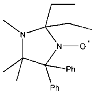	–[j]	0.57±0.15	0.38	–13.83[i]	–8.88	-[j]

[a] In benzene unless otherwise mentioned. [b] Given by eq 2 in ref 29. [c] $\sigma_{L,Me} = -0.01$, $\sigma_{L,Et} = -0.01$, $\sigma_{L,C(CH_2)_4} = 2\sigma_{L,Et} = -0.02$, $\sigma_{L,C(CH_3)_4} = 2\sigma_{L,Et} = -0.02$, $\sigma_{L,Ph} = 0.12$, $\sigma_{L,NMe_2} = 0.17$, $\sigma_{L,CMeNMe_2} = -0.01$, see refs 30 and 31. [d] r(Me) = 0.0, r(Et) = −0.38, see ref 29. [e] Given by eqs 3 and 5, see text. [f] Given by eqs 4 and 5, see text. [g] a_N for nitrogen hyperfine constant in mT in $CHCl_3$. [h] In acetonitrile. Thus a correcting factor of 2 times was applied to obtain k_c in benzene, see ref 14. [i] For $r(C(CH_2)_4)$, $r(C(CH_2)_5)$, $r(CH(CH_2)_4CH)$, r(*n*-Bu), and r(Ph), see text. [j] Not determined.

reactions of these nitroxides with alkyl radicals as well as overall suitability of these nitroxides for NMP has not yet been determined.

NMP[6] is one of the techniques for the synthesis of new block copolymers.[7] These materials have many applications in chemistry, physics, biology, and material science, and function as

SCHEME 1

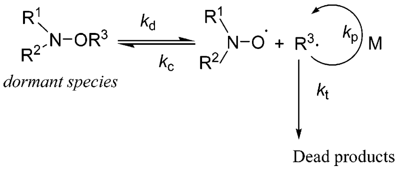

key building blocks in many areas of nanotechnology.[8] The simplest mechanism of NMP (Scheme 1) involves the reversible dissociation of a dormant nitroxyl end-capped polymer chain with rate constant k_d, the propagation of carbon-centered radicals k_p, the cross-coupling reaction between the nitroxide and the growing polymer chain with rate constant k_c, and the irreversible self-termination reactions of the carbon-centered radicals with rate constant k_t.

Several authors[9−12] have shown that for NMP to be efficient, the equilibrium constant $K = k_d/k_c$ should fall in the range from 10^{-7} to 10^{-11} mol L^{-1}. The values of k_d and k_c are sensitive functions of the alkoxyamine structure,[13,14] and knowledge of both the k_d and k_c values is crucial for successful control of polymer molecular weight. Recent efforts to improve the NMP technique have focused on the precise tuning of the reactivity of the corresponding radical species. It has been demonstrated that the introduction of bulky substituents on the nitroxide α-carbons may improve their suitability for NMP reactions. Thus, the development of new nitroxide mediators with higher k_d and not too low k_c values is an important endeavor. Such new mediators could be used not only in styrene polymerization, but also in the polymerization of methacrylates, acrylamides, and dienes.[15] In a recent paper, Siegenthaler and Studer[16] showed the importance of k_c on the efficiency of the polymerization. Thus, it is important to understand clearly the different processes and effects involved during the reformation of the alkoxyamines, and to have tools for predicting k_c values as for the homolysis of alkoxyamines. To date, there have only been two reports on the steric effects of the aminoxyl radical structure on the values of k_c.[17,18] Fischer et al.[17] observed a correlation between the energy of steric hindrance and coupling rate constants for the cross-coupling of the six-membered-ring piperazinone *N*-oxyl type radical and styryl radical. As far as we know, there are no extensive studies on the polar and the steric effects for the recombination between acrylate- and methacrylate-type radicals and nitroxide.

SCHEME 2

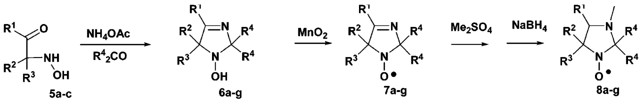

a) R^1 = Me, R^2 = R^3 = Et, 2R^4 = $(CH_2)_5$; b) R^1, R^4 = Me, R^2 = R^3 = Et; c) R^1+R^2 = $(CH_2)_4$, R^3 = Me, 2R^4 = $(CH_2)_5$; d) R^1 = R^2 = R^3 = Me, R^4 = Et; e) R^1,R^2,R^3 = Me, R^4 = *n*-Bu; f) R^1 = R^2 = R^3 = Me, 2R^4 = $(CH_2)_4$; g) R^1+R^2 = $(CH_2)_4$, R^3 = R^4 = Me.

In this work, we present the synthesis of new imidazolidine nitroxides **8a−g** and **12** (Table 1). The recognized preconditions for testing these particular nitroxides for NMP processes are that (i) there should exist low oxidation potentials for the imidazolidine nitroxides (in general they should be much lower than those of imidazolidine-3-ones)[19] and (ii) there should exist convenient methods for the synthesis of imidazolidine nitroxides with bulky substituents at positions 2 and 5 of the imidazole ring.[4] We applied the time-resolved chemically induced dynamic nuclear polarization (TR CIDNP) to determine the fate of the alkyl radicals R$^•$, (R = $C(CH_3)_2-C(O)OCH_3$ and $CH(CH_3)-C(O)-OtBu$) in the absence and in the presence of imidazolidine nitroxides. Then, the coupling rate constants between these two species were measured by laser flash photolysis (LFP) experiments. It is our goal to derive kinetic parameters for modeling NMP reactions, and to reveal the influence of steric and electronic factors upon these reactions. Within the series, the nitroxides we have studied differ in the steric and/or the electronic character of the functional groups surrounding the nitroxide moiety. The carbon-centered radicals were generated in the presence of the stable nitroxides by laser flash photolysis of the corresponding ketone precursors RC(O)R, whose photochemistry is well understood.[20] The rate constants of decomposition of alkoxyamines based on these series of nitroxides as well as polymerization results will be published elsewhere.

Results

Synthesis of Nitroxides. The nitroxides **8a−g** were synthesized in four steps, according to Scheme 2. The nitroxide **12** was prepared in four steps, according to the Scheme 3.

Time-Resolved CIDNP Experiments. The carbon-centered radicals MiB (methyl isobutyrate-2-yl) and tBP (*tert*-butyl propionate-2-yl) were generated by laser pulse photolysis of the appropriate symmetric ketones R−CO−R, as a propagating chain radical model formed for methyl methacrylate and *tert*-butyl acrylate polymerizations, respectively. The photochemistry and resulting ketone reaction paths are shown in Scheme 4.[14,21] After excitation of the n−π* transition and intersystem crossing, the ketones undergo α-cleavage from the triplet state to yield geminate (in-cage) acyl−alkyl radical pairs (reaction 1 in Scheme 4). The geminate reactions (reaction 2 in Scheme 4) of recombination and elimination of vicinal hydrogen result in the restoration of the initial ketone R−CO−R (I in Figure 1) and the formation of aldehyde R−CHO (V in Figure 1)) and alkene R(−H) (IV in Figure 1). The escaped acyl radicals undergo fast decarbonylation with the rate constant $k_{CO} = 2 \times 10^7$ s^{-1} for

---

(6) U.S. Patent 4,581,429. Solomon, D. H.; Rizzardo, E.; Cacioli, P. *Chem. Abstr.* **1985**, *102*, 221335q.

(7) Georges, M. K.; Veregin, R. P. N.; Kazmaier, P. M.; Hamer, G. K. *Macromolecules* **1993**, *26*, 2987−2988.

(8) *Nanoscale Science and Technology*; Kelsall, R. W., Hamley, I. W., Geoghegan, M., Eds.; John Wiley & Sons: Chichester, UK, 2005.

(9) Souaille, M.; Fischer, H. *Macromolecules* **2000**, *33*, 7378−7394 and references therein.

(10) Fischer, H.; Souaille, M. *Chimia* **2001**, *55*, 109−113 and references therein.

(11) Goto, A.; Fukuda, T. *Prog. Polym. Sci.* **2004**, *29*, 329−385.

(12) Greszta, D.; Matyjaszewski, K. *Macromolecules* **1996**, *29*, 7661−7670.

(13) Bertin, D.; Gigmes, D.; Marque, S.; Tordo, P. *Macromolecules* **2005**, *38*, 2638−2650.

(14) Beckwith, A. L. J.; Bowry, V. W.; Ingold, K. U. *J. Am. Chem. Soc.* **1992**, *114*, 4983−4992. Boury, V. W.; Ingold, K. U. *J. Am. Chem. Soc.* **1992**, *114*, 4992−4997. Chateauneuf, J.; Lusztyk, J.; Ingold, K. U. *J. Org. Chem.* **1988**, *53*, 1629−1630.

(15) Hawker, C. J.; Bosman, A. W.; Harth, E. *Chem. Rev.* **2001**, *101*, 3661−3688 and references therein.

(16) Siegenthaler, K. O.; Studer, A. *Macromolecules* **2006**, *39*, 1347−1352.

(17) Marque, S.; Sobek, J.; Fischer, H.; Kramer, A.; Nesvadba, P.; Wunderlich, W. *Macromolecules* **2003**, *36*, 3440−3442.

(18) Iwao, K.; Sakakibara, K.; Hirota, M. *J. Comput. Chem.* **1998**, *19*, 215−221.

(19) Chong, Y. K.; Ercole, F.; Moad, G.; Rizzardo, E.; Thang, S. H. *Macromolecules* **1999**, *32*, 6895.

(20) Turro, N. J. *Molecular Photochemistry*, 3rd ed.; Benjamin: Menlo Park, CA, 1974.

SCHEME 3

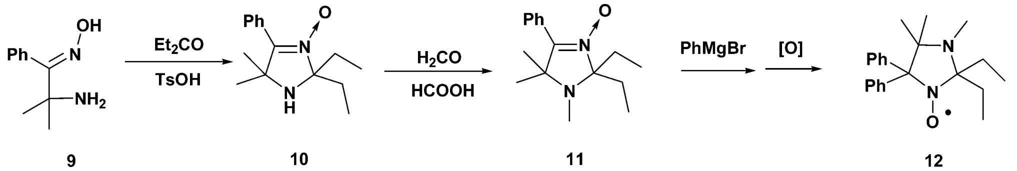

SCHEME 4

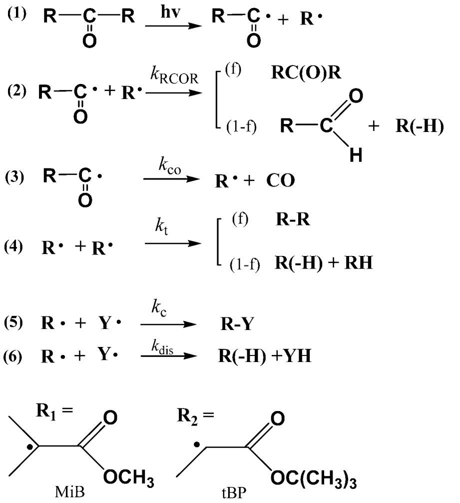

MiB[22] and $k_{CO} = 8 \times 10^6$ s^{-1} for tBP[23] (reaction 3 in Scheme 4). The consequent bulk reactions (reaction 4 in Scheme 4) of radical termination give rise to the formation of products R−R, RH, and R(−H) (II, III, and IV in Figure 1, respectively). In the presence of nitroxide these reactions are partly or entirely replaced by the coupling of carbon-centered radicals with the nitroxide and elimination of vicinal hydrogen from the carbon-centered radicals with the nitroxide (reactions 5 and 6 forming either hydroxylamine YH and alkene R(−H), or the stable adduct R−Y).[24] In general, this system is well suited for deriving coupling rate constants of alkyl radicals with nitroxides by means of either flash photolysis[21] or the switched external magnetic field CIDNP technique.[25,26]

In the high magnetic field of the NMR spectrometer the photolysis of either ketone leads to the formation of highly intensive CIDNP. The CIDNP spectrum obtained 100 μs after photolysis of Pest (see Experimental Section) in the absence of nitroxide is presented in Figure 1a. The phases of the CIDNP signals are the absorption for the initial compound R−CO−R (I in Figure 1) and the emission for the escape products R−R and RH (II and III in Figure 1, respectively), as predicted by Kaptein's rules[27] ($\Delta g > 0$, $A(CH_3) > 0$). The alkene R(−H) can be formed both in geminate reactions and in the bulk (IV in Figure 1). Therefore, immediately after the laser pulse the signal from the CH_3 group of R(−H) is in emission, which then decays on the microsecond time scale due to formation of absorptively polarized molecules in the bulk (this is the CIDNP cancellation effect[28]). In Figure 1, inserts above each signal show the kinetic behavior of the signals on the microsecond time scale.

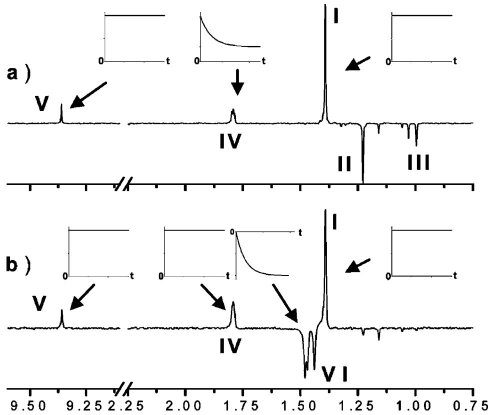

FIGURE 1. CIDNP spectra, obtained upon the photolysis of MiB in the absence (a) and in the presence (b) of nitroxide **8f**. Inserts: CIDNP kinetics of corresponding NMR lines in microsecond time scale. Peaks attribution: (I) MeOOC−C(CH_3)$_2$−C(O)−C(CH_3)$_2$−COOMe, (II) MeOOC−C(CH_3)$_2$−C(CH_3)$_2$−COOMe, (III) MeOOC−CH(CH_3)$_2$, (IV) MeOOC−C(CH_3)=CH$_2$, (V) MeOOC−C(CH$_3$)$_2$−C*H*O, and (VI) MeOOC−C(CH_3)$_2$−Y.

In the presence of nitroxides, both the CIDNP spectra and kinetics change significantly. Figure 1b shows the spectrum obtained 100 μs after laser flash photolysis of a 9 mM Pest (see Experimental Section) solution in the presence of 8 mM nitroxide **8f**. Strong emissive signals (VI in Figure 1b) are observed at 1.4−1.5 ppm, which corresponds to the CH_3 group of the coupling product R−Y resulting from the reaction of nitroxide and alkyl radicals. These signals show fast initial growth, but after 1−2 μs they practically do not change. The presence of the nitroxide inhibits the formation of bulk products R−R, RH, and R(−H), and this is indicated by the absence of any emissive bulk polarization in these products (Figure 1b). Generally, the reaction between alkyl radical R and nitroxide Y can proceed either via coupling (reaction 5, two diastereomers) or elimination of vicinal hydrogen (reaction 6). The absence of the bulk polarization at the products of reaction 6, R(−H) and YH, demonstrates that $k_c \gg k_{dis}$, and the main channel of the reaction between R$^\bullet$ and Y$^\bullet$ is the coupling. Similar results were obtained in CIDNP measurements performed with other nitroxides, as well as in the photolysis of tBest (see Experimental Section) with nitroxides.

The observed structure of CIDNP signals of RY (Figure 1b) indicates the existence of two diastereoisomers of the resulting coupling species with two unequivalent groups of methyl protons in each of them. This fact is confirmed by NMR spectra of corresponding alkoxyamines. Thus, the CIDNP study shows the

---

[21] Sobek, J.; Martschke, R.; Fischer, H. *J. Am. Chem. Soc.* **2001**, *123*, 2849−2857.

[22] Tsentalovich, Y. P.; Fischer, H. *J. Chem. Soc., Perkin Trans. 2* **1994**, 4, 729−733.

[23] Schuh, H.; Fischer, H. *Helv. Chim. Acta* **1978**, *61*, 2463.

[24] Ananchenko, G.; Fischer, H. *J. Chem. Soc., Perkin Trans. 2* **2001**, 1887−1889.

[25] Bagryanskaya, E. G.; Gorelik, V. R.; Sagdeev, R. Z. *Chem. Phys. Lett.* **1997**, *264*, 655.

[26] Lebedeva, N. V.; Zubenko, D. P.; Bagryanskaya, E. G.; Ananchenko, G. S.; Marque, S.; Tordo, P.; Sagdeev, R. Z. *Phys. Chem. Chem. Phys.* **2004**, *6*, 2254−2259.

[27] Salikhov, K. M.; Molin, Y. N.; Sagdeev, R. Z.; Buchachenko, A. L. *Spin polarization and magnetic effects in radical reactions*; Elsevier: Amsterdam, The Netherlands, 1984.

[28] Vollenweider, J.-K.; Fischer, H.; Hennig, J.; Leuschner, R. *Chem. Phys.* **1985**, *97*, 217−234.

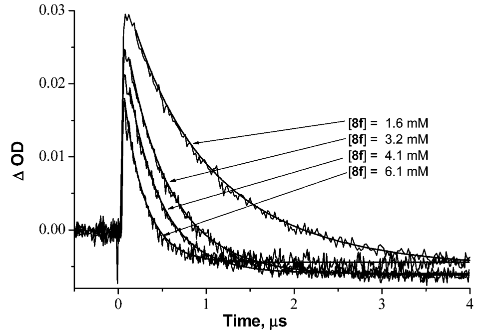

FIGURE 2. Time dependence of the methyl isobutyrate radical absorption at 325 nm in benzene (room temperature, various concentrations) and in the presence of **8f**.

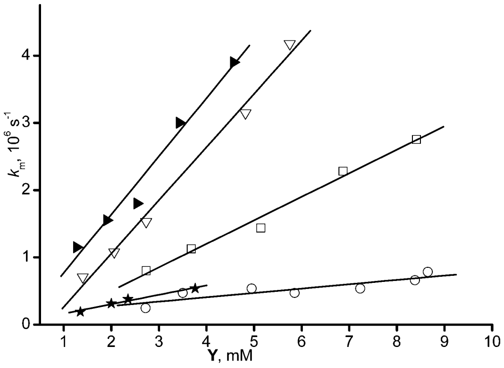

FIGURE 3. Concentration dependence of the apparent rate constant k_m for the cross-coupling of MiB with nitroxides in benzene at room temperature: (▲) for **1**, (▽) for **2**, (☐) for **4**, (★) for **8b**, and (○) for **8f**.

effective coupling reaction of a series of imidazolidine nitroxides with alkyl radicals.

The rate constants k_c of radical cross-termination (reaction 4) were determined by using laser flash photolysis. Alkyl radicals R were generated by 308 nm pulse photolysis of the corresponding ketones, and their decays were monitored at the absorption maximum of 325 nm. The acrylate radical absorption spectrum has been measured by Sobek et al.[21] In the absence of nitroxides, the carbon-centered radicals decay by second-order kinetics with $k_t/\epsilon = 4.7 \times 10^6$ cm/s for MiB and $k_t/\epsilon = 1.9 \times 10^6$ cm/s for tBP, where ϵ is the extinction coefficient of the corresponding alkyl radical. With added nitroxide, their decay accelerates and becomes pseudo-first-order decay (Figure 2) according to step 5 in Scheme 4. Typically, our measurements were performed with at least four different concentrations of nitroxides. To separate the exponential contribution into signal decay, the kinetic traces were obtained with 4−5 different intensities of the laser pulse for each solution. The observed pseudo-first-order rate constant k_m was found to be proportional to the nitroxide concentration, $k_m = k_0 + k_c[Y]$ (k_0 for the side reactions). Some typical kinetics obtained from these measurements are shown in Figure 3, and the calculated values of k_c are listed in Table 1.

For cross-reaction of nitroxides **1** and **3** with MiB, rate constants were measured over a considerable temperature range (300−370 K) and data are shown in Figure 4.

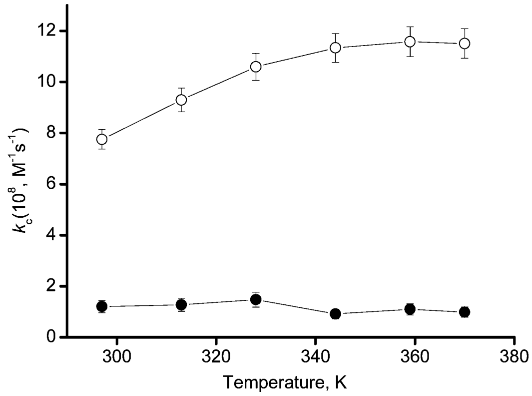

FIGURE 4. Temperature dependence of the cross-coupling rate constant of the carbon-centered radical MiB with nitroxides **1** (○) and **3** (●).

The Multiparameter Approach. As we mentioned in the Introduction, to date, there have only been two reports on steric effects of the nitroxide structure on the values of k_c.[17,18] Fischer et al.[17] showed that the steric effect of substituents on the α positions of the piperazinone *N*-oxyl moiety is expressed by eq 1 with E_s, the steric constant, and r_i, the individual steric constants of each substituent. In the same paper, it was shown that k_c is linearly correlated to $E_{s,n}$ (eq 2), the steric constant of the whole molecule.

$$E_s(R_1R_2R_3C) = -2.104 + 3.429r_1(R_1) + 1.978r_2(R_2) + 0.649r_3(R_3) \quad (1)$$

$$\log(k_c/M^{-1}\,s^{-1}) = \log(k_{c,0}/M^{-1}\,s^{-1}) + \delta E_{s,n} \quad (2)$$

It has to be mentioned that the larger the group, the more negative r_i, thus r_1 is for the small group, r_2 for the medium group, and r_3 for the large group. In his paper, Fischer did not determine the cyclic steric constant, and thus assumed all the possibilities for the size of the ring.[17] Our series is too small, and the alkyl radicals studied are very different from the styryl radical studied by Fischer et al.,[17] therefore the cyclic strain for the five-membered ring is not determined. The cyclic steric constant r(C5) is set in the first position when assumed larger than the methyl group, that is, $E^1{}_s$ is given by eq 3. When the cyclic steric constant is assumed between that of the methyl and the ethyl groups, the steric constant is also given by $E^1{}_s$. The r(C5) is set in the third position when it is assumed smaller than r(Et), that is, $E^3{}_s$ is given by eq 4.

$$E^1{}_s = -2.104 + 3.429r(C5) + 1.978r_2(R_2) + 0.649r_3(R_3) \quad (3)$$

$$E^3{}_s = -2.104 + 3.429r_1(R_1) + 1.978r_2(R_2) + 0.649r(C5) \quad (4)$$

It was also assumed that the steric constant of the molecule $E_{s,n}$ is given by the sum of the steric constant of substituent in positions 2 and 5 (eq 5).[29]

$$E_{s,n} = E_s(R_1R_2R_3C2) + E_s(R_1R_2R_3C5) \quad (5)$$

The values of k_c for **2** and **8e** are close to k_c of **8d** and indicate that the steric demands of the *spiro*-cyclohexyl moiety and geminal *n*-butyl groups are close to the steric demand of the geminal ethyl groups. This is also observed for **8a** and **3**. The same remarks hold for the *spiro*-cyclopentyl moiety in the

---

(29) Marque, S. *J. Org. Chem.* **2003**, *68*, 7582−7590.

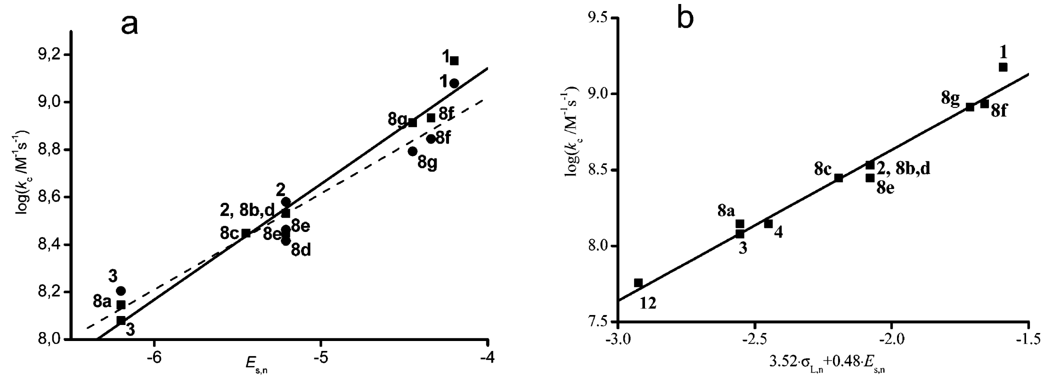

FIGURE 5. (a) Log(k_c/M^{-1} s^{-1}) vs $E_{s,n}$ estimated by using E_s^1 for **1**−**3** and **8** nitroxides: (■, —) for MiB radical, (●, - - -) for tBP radical. (b) Log(k_c/M^{-1} s^{-1}) vs Linear combination of molecular descriptors ($\sigma_{L,n}$ and $E_{s,n}$) for **1**−**4**, **8a**−**g**, and **12** nitroxides and the MiB alkyl radical.

TABLE 2. Coefficients for Eq 2 Depending on Both Alkyl Radicals MiB and TBP and the Steric Constants E^1_s and E^3_s

alkyl radicals	eqs	log $k_{c,0}$[a]	δ	N[b]	s[c]	R^2[d]	t[e]
tBP	6[f]	10.64 ± 0.29	0.41 ± 0.06	7	0.10	0.91	99.91
	7[g]	9.80 ± 0.17	0.20 ± 0.03	7	0.10	0.91	99.92
MiB	8[f]	11.09 ± 0.17	0.49 ±0.07	10	0.08	0.96	99.99
	9[g]	10.06 ± 0.11	0.24 ± 0.02	10	0.08	0.96	99.99

[a] Value for the *y*-intercept and corresponding to the nitroxides exhibiting no steric effect (E_s = 0.0). [b] Number of data. [c] Standard deviation. [d] Square of the regression coefficient. [e] Student *t*-test given in percent. [f] For $E_{s,n}$ given by eqs 3 and 5. [g] For $E_{s,n}$ given by eqs 4 and 5.

nitroxide **8f** and geminal methyl groups in nitroxide **1**. The lack of steric effect of the linear alkyl chain has already been reported.[29] The six-membered ring formed by junction between positions 4 and 5 of the imidazolidin *N*-oxyl radical is assumed to exhibit the same steric demand as the ethyl group. Then, the steric effect on the coupling reaction of **1**−**4** and **8a**−**g** with tBP and MiB was correlated to k_c via eqs 2 and 5, and good correlations are observed for both possibilities E^1_s and E^3_s (Table 1, Figure 5a, eqs 6−9 in Table 2). The statistical outputs are good for both possibilities and confirm the monotonic increase of k_c with the steric demand around the nitroxyl moiety.

The steric constants E^1_s and E^3_s for **4** and **12** were estimated by assuming that the steric effect of the β substituents (two methyl groups in position 4 of the imidazolidine ring) is the same as for the series **1**−**4** and **8a**−**g** (one methyl group), and assuming a value of −1.40 for the steric constant r_i of the phenyl group.[26] It has been shown[26] that a biparametric equation—polar effect and stabilization of the nitroxide accounted for by the electrical Hammett constant σ_L, and the steric effect of the substituents around the nitroxide moiety accounted for by the steric constant E_s—described the effects influencing the C−ON bond homolysis rate constant k_d. Therefore, it was assumed that the same effects—polar and steric effects of the substituents around the nitroxide moiety, and the stabilization of the nitroxide—influence increases the coupling rate constants k_c. The electron-withdrawing effect of the substituents should increase the spin density on the nitroxide oxygen atom and, thereby, should enhance the reactivity of nitroxide in the coupling reaction by increasing the contribution of resonance form **A** (Scheme 5).

Therefore, such an effect accounted for by the electrical Hammett constant σ_L would increase k_c, i.e., a positive ρ coefficient should be observed in eq 10. It was expected that the steric effect due to the substituents in position α,α′ of the nitroxide moiety would hamper the approach of the alkyl radical and thus destabilize the transition state, i.e., a positive δ coefficient should be observed in eq 10.

SCHEME 5

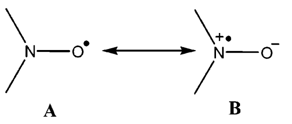

$$\log(k_c/\mathrm{M}^{-1}\,\mathrm{s}^{-1}) = \rho\sigma_{L,n} + \delta E_{s,n} + \log(k_{c0}/\mathrm{M}^{-1}\,\mathrm{s}^{-1}) \qquad (10)$$

The statistical outputs for biparametric regression are very good (Student *t*-test above 99.99%), and the coefficients are positive (eq 11) as expected for the coupling of nitroxides **1**−**4**, **8a**−**g**, and **12** and the MiB radical when E^1_s is used to estimate $E_{s,n}$.

$$\log(k_c/\mathrm{M}^{-1}\,\mathrm{s}^{-1}) = 3.52(\pm 0.43)\sigma_{L,n} + 0.47(\pm 0.03)E_{s,n} + 10.62(\pm 0.12) \qquad (11)$$

for R^2 = 0.98, N = 12, s = 0.07, and $F_{11,99.99\%}$ = 191.

The statistical outputs are as good when E^3_s is applied, assuming r(C5) is smaller than r(Ph), which is highly improbable. Other possible combinations afforded poorer statistical outputs.

Discussion

The values of cross-coupling rate constants of different nitroxides k_c summarized in Table 1 are markedly below the diffusion-controlled limit of about 5×10^9 M^{-1} s^{-1}, and depend very slightly on temperature, showing very small, or even negative, activation energy. The same dependence previously has been observed for the series of stable nitroxides by several authors.[18,14] In general, radical coupling reactions exhibit very low E_a values, i.e., below 10 kJ/mol. Therefore, the variation of k_c with T is weak (see Arrhenius equation). This indicates the entropy control of the reaction, i.e., hampered approach of the alkyl radical to the oxygen centered radical.[14,18]

In general, coupling rate constants decrease with increasing steric congestion of the reactive center of the nitroxides. As mentioned above, Fischer et al.[17] observed a correlation between $E_{s,n}$ and log k_c for the cross-coupling of six-membered-ring piperazinone *N*-oxyl type radical and the 1-phenylethyl alkyl radical. With the series **1**−**3** and **8a**−**g**, which exhibits the same polar effect, the linear relationship between $E_{s,n}$ and log k_c

(eq 7 in Table 1) for the coupling of MiB and tBP alkyl radicals exemplifies the generality of this approach, that is, the k_c values decrease with increasing congestion around the nitroxyl moiety. Interestingly, as the steric effect is mainly contained in the activation entropy $\Delta S^\ddagger$ (vide supra), it means that $\Delta S^\ddagger$ increases monotonically with the size of the substituents in the position α,α′. It is worthy to mention, as the slopes of eqs 6−9 (Table 2, Figure 5a) are very close, that the values of k_c depend only slightly on the type of alkyl radicals, propanoate-2-yl (acrylate type) and 2-methylpropanoate-2-yl (methacrylate type) alkyl radicals.

Very good biparametric correlation with positive slope ρ (Figure 5b, eq 11) was observed when molecules **4** and **12**, exhibiting different σ_L values,[30,31] were included in the series, meaning that increasing polar/destabilization effect increased k_c. Assuming negligible polar effect in the transition state, electron-withdrawing groups favor the form **A** over the form **B** in the initial state—the form **B** is destabilized for electron-withdrawing groups attached to the nitrogen atom—thus the relocation of the odd-electron on the oxygen atom is easier, and hence, the activation barrier ($\Delta H^\ddagger$ or E_a) is lower. This destabilization is denoted by changes in activation enthalpy $\Delta H^\ddagger$, which decreases with increasing σ_L values. Therefore, it is remarkable that eq 11 takes into account the effects occurring both in the transition state and in the initial state, and involving simultaneous changes in $\Delta S^\ddagger$ and $\Delta H^\ddagger$. The increasing k_c with increasing σ_L values means the coupling reaction is facilitated by the presence of electron-withdrawing groups close to the nitroxyl function. It is worthwhile to mention that the polar effect is rather important (35%) to the steric effect (65%).[32]

Conclusions

All the results concur with the exclusive coupling of acrylate- and methacrylate-type radicals with the imidazolidine nitroxides. Furthermore, we showed that the approach proposed by Fischer et al.[17] to account for the steric effect is versatile enough to be applied to other alkyl radicals such as MiB and tBP radicals. With the series **1−4**, **8a−g,** and **12**, we showed that the polar effect exerts significant influence on k_c. Consequently, for developing a new nitroxide efficient in NMP it might be interesting to change the scavenging properties by varying the polarity of the substituents and keeping the same steric hindrance. The suitability of the synthesized series of nitroxides for NMP is under investigation, i.e., measurement of k_d and polymerization experiments.

Experimental Section

Materials. Ketone concentrations were 20 mM in the case of 2,4-dimethyl-3-oxopentanedioic acid di-*tert*-butyl ester (tBEst) and 2,2,4,4-tetramethyl-3-oxopentanedioic acid dimethyl ester (Pest). The concentrations of nitroxides were varied from 2 to 10 mM. The ketones were synthesized according to refs 33 and 34 and purified by column chromatography. The solvents (benzene and acetonitrile) were distilled prior to use. The IR spectra were recorded on an FT-IR spectrometer in KBr pellets (the concentration was 0.25%; the pellet thickness was 1 mm). The UV spectra were measured in EtOH. The ^{1}H NMR spectra were recorded on a 300 MHz NMR spectrometer for 5% solutions, using the signal of the solvent as the standard. The ^{13}C NMR spectra were recorded on 75 and 100 MHz NMR spectrometers for 5−10% solutions at 300 K, using the signal of the solvent as the standard. The assignment of the signals in the ^{13}C NMR spectra was made based on analysis of intensities, on the spectra measured in *J*-modulation mode, and using the data reported previously.[4] High-resolution mass spectra were recorded and element analyses were performed.

The nitroxides **1−4** (see Table 1) were prepared according to the methods described in refs 4 and 35−37, respectively. The nitroxides **7f** and **7g** were prepared according to the methods described in refs 38 and 39, respectively.

2,2-Diethyl-3-methyl-1,4-diazaspiro[4,5]dec-3-en-1-ol (6a). A suspension of 3-hydroxyamino-3-ethylpentan-2-one hydrochloride **5a**[4] (5 g, 27.5 mmol) and ammonium acetate (7.7 g, 100 mmol) in a mixture of cyclohexanone (10 mL, 93 mmol) and methanol (8 mL) was stirred under argon for 24 h. The resulting solution was poured into water (20 mL), basified with $NaHCO_3$, and extracted with diethyl ether (3 × 10 mL). The ether layers were thoroughly washed with water (5 × 10 mL) and dried over Na_2CO_3. The ether was removed under reduced pressure, the residue was triturated with hexane at −5 °C, and the crystalline precipitate of **6a** was filtered off and washed with hexane, yielding 3.8 g, 60%, of colorless crystals, mp 129−133° (hexane) (Found: C, 69.54; H, 10.48; N, 12.44. Calcd for $C_{13}H_{24}N_2O$: C, 69.60; H, 10.78; N, 12.49); ν_{max} (KBr)/cm^{-1} 2924, 2870, 1655, 1472, 1451, 1428, 1384, 1282, 1266, 1175, 1034, 962, 934, 900, and 851; δ_H (200 MHz; $CDCl_3$) 0.85 (6 H, br t, $J = 7$ Hz, 2 × CH_3, Et), 1.23−1.87 (14 H, br m, 7CH_2), 1.90 (3 H, s, $CH_3C{=}N$), and 6.00 (1 H, br s, OH); δ_C (50 MHz; $CDCl_3$) 8.8 (CH_3, Et), 27.1 (CH_2, Et), 25.0, 22.8, and 35.6 ($(CH_2)_5$), 16.2 ($\mathit{C}H_3{-}C{=}N$), 78.2 (C^5), 91.4 (C^2), and 171.2 ($C{=}N$).

2,5-Dihydroimidazol-1-ols **6b−e** were prepared in a similar manner from 3-hydroxyamino-3-methylbutane-2-one hydrochloride **5b**,[40] 3-hydroxyamino-3-ethylpentan-2-one hydrochloride **5a**, and 2-hydroxyamino-2-methylcyclohexanone hydrochloride **5c**[40] and the corresponding ketones (acetone, diethyl ketone, cyclohexanone, and dibutyl ketone) at 25 °C or under reflux (for **6c**) for 3 h to 7 days, until hydroxyaminoketone was completely reacted (the sample was basified with 25% NH_3 and analyzed with use of TLC Silufol; eluent: diethyl ether). The reaction mixtures were cooled to 5 °C, and the precipitates of **6b−e** were filtered off and washed with water.

2,2,4-Trimethyl-5,5-diethyl-2,5-dihydroimidazol-1-ol (6b). Yield 80%, colorless crystals, mp 114−118 (hexane) (Found: C, 65.04; H, 10.80; N, 15.37. Calcd for $C_{10}H_{20}N_2O$: C, 65.18; H, 10.94; N, 15.20); ν_{max} (KBr)/cm^{-1} 3172 (br), 2977, 2925, 2880, 1661, 1465 (br), 1434, 1373, 1263, 1232, 1200, 1036, and 877; δ_H (400 MHz; $CDCl_3$) 0.85 (6 H, t, $J = 7$ Hz, 2 × CH_3, Et), 1.37 (6H, s, 2Me), 1.58 and 1.70 (each 2 H, m, 2CH_2), 1.86 (3 H, s, $CH_3C{=}N$), and 6.65 (1 H, br s, OH); δ_C (100 MHz; $CDCl_3$) 5.3 (CH_3, Et), 12.8 ($\mathit{C}H_3{-}C{=}N$), 22.5 (CH_2, Et), 22.6 ($\mathit{C}H_3$), 75.5 (C5), 86.5 (C2), and 168.0 ($C{=}N$).

---

(30) Charton, M. *Prog. Phys. Org. Chem.* **1981**, *13*, 119−251.

(31) Charton, M. In *Advances in Quantitatives Structure−Property Relationship*; Charton, M., Ed.; Jai Press Inc.: Greenwich, CT, 1996; Vol. 1, pp 171−219.

(32) The weigth of each effect was estimated with equations given in: Shorter, J. In *Correlation Analysis of Organic Reactivity*; Research Studies Press: Chichester, UK, 1982; pp 73−126.

(33) Favorski, A. E.; Umnova, A. *J. Prakt. Chem. II* **1912**, *88*, 679.

(34) Knühl, B.; Marque, S.; Fischer, H. *Helv. Chim. Acta* **2001**, *84*, 2290.

(35) Volodarski, L. B.; Reznikov, V. A.; Kobrin, V. S. *J. Org. Chem. USSR* (*Engl. Transl.*) **1979**, *13*, 364.

(36) Reznikov, V. A.; Volodarsky, V. A. *Izv. Sib. Otd. Akad. Nauk SSR, Ser. Khim. Nauk* **1984**, *8*, 89−97 (in Russian); *Chem. Abstr.* **1985**, *102*, 6297y.

(37) Martin, V. V.; Volodarsky, V. A.; Vishnivetskaya, L. A. *Izv. Sib. Otd. Akad. Nauk SSSR, Ser. Khim. Nauk* **1981**, *4*, 94−103 (in Russian); *Chem. Abstr.* **1982**, *96*, 6648y.

(38) Sevastjanova, T. K.; Volodarsky, L. B. *Bull. Acad. Sci. USSR Div. Chem. Sci.* (*Engl. Transl.*) **1972**, *21*, 2276.

(39) Volodarsky, L. B.; Kutikova, G. A. *Bull. Acad. Sci. USSR Div. Chem. Sci.* (*Engl. Transl.*) **1971**, *20*, 859−863.

(40) Volodarsky, L. B.; Sevastjanova, T. K. *Zh. Org.Khim.* **1971**, *8*, 1687 (in Russian); *Chem. Abstr.* **1971**, *75*, 140425r.

Methyl-5,6,7,7a-tetrahydrospiro[benzimidazole-2,1′-cyclohexan]-1(4*H*)-ol (6c). Yield 32%, colorless crystals, mp 175−177 °C (ethyl acetate−heptane 1:1) (Found: C, 68.41; H, 9.97; N, 11.99. Calcd for $C_{13}H_{22}N_2O \cdot {}^1/_3H_2O$: C, 68.38; H, 10.01; N, 12.27); ν_{max} (KBr)/cm^{-1} 3171 (br), 2937, 2859, 1655, 1368, 1285, 1206, 1081, 1029, 983, 957, and 911; δ_H (200 MHz; $CDCl_3$) 1.45 (3 H, s, Me), 1.60−2.80 (18 H, br m, 9 × CH_2), and 6.45 (1 H, br s, OH); δ_C (50 MHz; $CDCl_3$) 15.0 (CH_3), 88.9 (C1′), 67.2 (C5), 37.3 (C6), 34.2 (C2′), 30.4 (C6′), 26.1 (C9), 22.9 (C4′), 21.8 (C8), 19.9 (C7), 19.2 (C3′), 18.6 (C5′), and 172.0 (C═N).

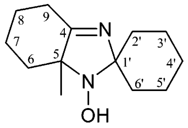

2,2-Diethyl-4,5,5-trimethyl-2,5-dihydro-1*H*-imidazol-1-ol (6d). Reaction conditions: 40 °C for 3 h under argon. Yield 65%, colorless crystals, mp 130−132 °C (hexane) (Found: C, 64.94; H, 10.87; N, 14.85. Calcd for $C_{10}H_{20}N_2O$: C, 65.18; H, 10.94; N, 15.20); ν_{max} (KBr)/cm^{-1} 3166 (br), 2966, 2934, 2877, 1656, 1464, 1432, 1378, 1224, 1035, 957, and 931; δ_H (400 MHz; $CDCl_3$) 0.87 (6 H, br t, J = 7 Hz, 2 × CH_3, Et), 1.23 (6H, s, 2Me,), 1.63 and 1.84 (each 2 H, br m, 2 × CH_2, Et), 1.95 (3 H, s, CH_3C═N), and 6.60 (1 H, br s, OH); δ_C (100 MHz; $CDCl_3$) 6.8 (CH_3, Et), 14.1 (CH_3−C═N), 21.8 (CH_3), 27.4 (CH_2, Et), 70.2 (C5), 92.8 (C2), and 173.0 (C═N).

2,2-Dibutyl-4,5,5-trimethyl-2,5-dihydro-1*H*-imidazol-1-ol (6e). Yield 30%, colorless crystals, mp 115−117 °C (hexane) (Found: C, 70.11; H, 11.83; N, 11.65. Calcd for $C_{14}H_{28}N_2O$: C, 69.95; H, 11.74; N, 11.65); ν_{max} (KBr)/cm^{-1} 3169, 2960, 2932, 2871, 1655, 1467, 1226 1032, 1016, 982, and 956; δ_H (400 MHz; $CDCl_3$) 0.87 (6 H, br t, J = 7 Hz, 2 × CH_3, n-Bu), 1.25 (6H, s, 2Me), 1.29 (m, 8H, 4 × CH_2), 1.59 and 1.80 (each 2 H, br m, 2 × CH_2, C2−CH_2), 1.96 (3 H, s, CH_3C═N), and 6.50 (1 H, br s, OH); δ_C (100 MHz; $CDCl_3$) 12.6 (CH_3, Bu), 14.4 (CH_3−C═N), 22.1 (CH_3), 21.85, 24.9, and 35.5 (CH_2, *n*-Bu), 70.5 (C5), 92.7 (C2), and 172.8 (C═N).

2,2-Diethyl-3-methyl-1,4-diazaspiro[4,5]dec-3-en-1-oxyl (7a). Manganese dioxide (2 g, 23 mmol) was added to a stirred solution of **6a** (1 g, 4.5 mmol) in chloroform (20 mL). The suspension was stirred for 0.5 h, manganese oxides were filtered off, and filtrate was evaporated under reduced pressure to leave orange crystalline solid, which was purified by column chromatography on silica (Kieselgel 60, Merck; eluent: diethyl ether:hexane 1:20) to yield nitroxide **7a** (0.95 g, 95%), orange crystals, mp 86−88 (hexane) (Found: C, 69.89, H, 10.32; N, 12.41. Calcd for $C_{13}H_{23}N_2O$: C, 69.9; H, 10.4; N, 12.5); ν_{max} (KBr)/cm^{-1} 2972, 2961, 2935, 2853, 1637, 1452, 1423, 1386, 1376, 1356, 1325, 1294, 1263, 1210, 1172, 1142, 1109, 962, 933, 912, 845, and 813.

The nitroxides **7b**−**e** were prepared with the same procedure.

2,2,4-Trimethyl-5,5-diethyl-2,5-dihydroimidazol-1-oxyl (7b). Yield 90%, orange oil (Found: C, 65.92, H, 10.73; N, 14.93. Calcd for $C_{13}H_{21}N_2$: C, 65.54; H, 10.45; N, 15.29); ν_{max} (KBr)/cm^{-1} 2979, 2930, 2880, 1638, 1458, 1429, 1381, 1357, 1266, 1249, 1199, 1186, 953, 935, 869, and 843; *m*/*z*, found 183.14892, calcd for $C_{10}H_{19}N_2O$ 183.14973.

7a-Methyl-5,6,7,7a-tetrahydrospiro[benzimidazole-2,1′-cyclohexan]-1(4*H*)-oxyl (7c). Yield 36%, orange crystals, mp 95−97 °C (hexane) (Found: C, 70.19, H, 9.72; N, 12.44. Calcd for $C_{13}H_{21}N_2O$: C, 70.55; H, 9.56; N, 12.66); ν_{max} (KBr)/cm^{-1} 2980, 2940, 2856, 1648, 1461, 1448, 1372, 1288, 1160, 962, and 907; *m*/*z*, found 222.17289, calcd for $C_{13}H_{21}N_2O$ 222.17320.

2,2-Diethyl-4,5,5-trimethyl-2,5-dihydroimidazol-1-oxyl (7d). Yield 90%, orange oil (Found: C, 65.86, H, 10.23; N, 15.12. Calcd for $C_{10}H_{19}N_2O$: C, 65.54; H, 10.45; N, 15.29); ν_{max} (neat)/cm^{-1} 2976, 2938, 2881, 1642, 1462, 1430, 1377, 1167, 953, and 928.

2,2-Dibutyl-4,5,5-trimethyl-2,5-dihydroimidazol-1-oxyl (7e). Yield 90%, orange oil; ν_{max} ($CHCl_3$, 2%)/cm^{-1} 2960, 2934, 2873, 1643, 1466, 1428, 1380, 1238, and 1159; *m*/*z*, found 239.21217, calcf for $C_{14}H_{27}N_2O$ 239.21233.

2,2-Diethyl-3,4-dimethyl-1,4-diazaspiro[4,5]decan-1-oxyl (8a). Dimethyl sulfate (0.5 g, 4 mmol) was added to a solution of **7a** (0.5 g, 2.4 mmol) in dry diethyl ether (3 mL). The solution was allowed to stand for 0.5 h at 25 °C and filtered, then diethyl ether was removed under reduced pressure. The residue was heated to 50 °C for 30 min under reduced pressure and then triturated with dry diethyl ether to form a highly hygroscopic yellow crystalline precipitate of quaternary salt. The precipitate was filtered off (without drying), washed with dry diethyl ether, and immediately dissolved in ethanol (5 mL). $NaBH_4$ (150 mg, 4 mmol) was added to the solution and the mixture was stirred for 1 h. Ethanol was removed under reduced pressure, and the residue was dissolved in water (2 mL) and extracted with diethyl ether (3 × 2 mL). The extract was dried over Na_2CO_3, then diethyl ether was removed under reduced pressure to leave a yellow oil, which was purified by column chromatography on silica (Kieselgel 60 Merck, eluent diethyl ether:hexane 1:20) to yield the nitroxide **8a** (480 mg, 90%) as a yellow oil (Found: C, 70.11; H, 11.68; N, 11.49. Calcd for $C_{13}H_{27}N_2O$: C, 70.24; H, 11.37; N, 11.70); ν_{max} (neat)/cm^{-1} 2972, 2934, 2859, 2792, 1448, 1420, 1382, 1351, 1297, 1264, 1233, 1216, 1201, 1139, 1079, 1064, 1036, 965, 922, 907, 868, 846, and 788.

The nitroxides **8b**−**g** and **12** were prepared by the same procedure.

5,5-Diethyl-2,2,3,4-tetramethylimidazolidin-1-oxyl (8b). Yield 90%, yellow oil (Found: C, 66.64, H, 11.63; N, 13.98. Calcd for $C_{11}H_{23}N_2O$: C, 66.29; H, 11.63; N, 14.05); ν_{max} (neat)/cm^{-1} 2978, 2938, 2881, 2848, 2796, 1461, 1383, 1368, 1355, 1271, 1239, 1170, 965, 922, and 887; *m*/*z*, found 199.18070, calcd for $C_{11}H_{23}N_2O$ 199.18103.

3,7a-Dimethylhexahydrospiro[benzimidazole-2,1′-cyclohexan]-1(3*H*)-oxyl (8c). Yield 30%, orange oil (Found: C, 71.07; H, 10.54; N, 11.63. Calcd for $C_{14}H_{25}N_2O$: C, 70.84; H, 10.62; N, 11.80); ν_{max} (neat)/cm^{-1} 2977, 2960, 2939, 2860, 1463, and 1445.

2,2-Diethyl-3,4,5,5-tetramethylimidazolidin-1-oxyl (8d). Yield 60%, orange oil (Found: C, 66.34; H, 11.38; N, 14.08. Calcd for $C_{11}H_{23}N_2O$: C, 66.29; H, 11.63; N, 14.05); ν_{max} (neat)/cm^{-1} 2978, 2935, 2879, 2851, 2795, 1452, 1376, 1361, 1337, 1226, 1203, and 969; *m*/*z*, found 199.18070, calcd for $C_{11}H_{23}N_2O$ 199.18103.

2,2-Dibutyl-3,4,5,5-tetramethylimidazolidin-1-oxyl (8e). Yield 70%, orange oil, ν_{max} (neat)/cm^{-1} 2956, 2971, 2870, 2791, 1473, 1451, 1375, 1361 and 1254; *m*/*z*, found: 255.24315, calc. for $C_{15}H_{31}N_2O$: 255.24362.

2,2,3,4-Tetramethyl-1,4-diazaspiro[4.4]nonan-1-oxyl (8f). Yield 48%, orange oil; ν_{max} (neat)/cm^{-1} 2956, 2871, 2794, 1468, 1453, 1378, 1360, 1336, 1263, 1207, 1191, 1144, 1067, and 1036; *m*/*z*, found 197.16529, calcd for $C_{11}H_{21}N_2O$ 197.16538.

2,2,3,7a-Tetramethyloctahydro-1*H*-benzimidazol-1-oxyl (8g). Yield 60%, orange oil (Found: C, 66.24; H, 10.42; N, 14.63. Calcd for $C_{11}H_{21}N_2O$: C, 66.29; H, 10.73; N, 14.20); ν_{max} (neat)/cm^{-1} 2976, 2935, 2859, 2796, 2738, 1463, 1445, 1369, 1274, 1242, 1208, 1174, and 993.

2,2-Diethyl-5,5-dimethyl-4-phenyl-2,5-dihydro-1*H*-imidazole 3-oxide (10). A solution of 2-amino-2-methyl-1-phenylpropan-1-one oxime (**9**)[41] (3.56.g, 20 mmol) and *p*-toluenesulfonic acid (86 mg, 0.5 mmol) in pentane-3-one (5 mL, 60 mmol) was stirred at 90 °C for 120 h. The mixture was separated by column chromatography on silica (Kieselgel 60, Merck, chloroform as eluent) to yield 1.4.g (28%) of **10**, as colorless crystals, mp 77−79 (hexane) (Found: C, 73.03; H, 9.45; N, 11.43. Calcd for $C_{15}H_{22}N_2O$: C, 73.13; H, 9.00; N, 11.37); ν_{max} (KBr)/cm^{-1} 3257, 2977, 2961, 2934, 2876, 1587, 1569, 1497, 1462, 1358, 1266, 1222,

---

[41] Volodarskii, L. B.; Tormyshewa, N. Y. *Izv. Sib. Otd. Akad. Nauk SSSR. Ser. Khim. Nauk.* **1976**, *4*, 136 (in Russian); *Chem. Abstr.* **1976**, *85*, 159592.

1203, 1166, 1046, 1016, 807, and 759; λ_{max} (EtOH)/nm 284 (log ϵ 3.79); δ_H (400 MHz; $CDCl_3$) 0.94 (6 H, t, $J = 7$ Hz, $2CH_3$, Et), 1.55 (6 H, s, $2CH_3$), 1.84 and 1.97 (both 2 H, m, 2 × CH_2), 7.0 (3 H, m, Ph-*m*,*p*), and 8.05 (2 H, m, Ph-*o*); δ_C (75 MHz; $CDCl_3$) 7.6 (CH_3, Et), 29.8 (5-CH_3), 30.0 (CH_2, Et), 62.0 (C5), 93.5 (C2), 142.5 (C4), Ph: 128.0 (C−*i*), 128.3 (C−*o*), 127.6 (C−*m*), and 129.5 (C−*p*).

2,2-Diethyl-1,5,5-trimethyl-4-phenyl-2,5-dihydro-1*H*-imidazole 3-Oxide (11). Formic acid, 90% (1.5 mL, 35 mmol), was added portionwise to a solution of **10** (1.3 g, 5.2 mmol) in an aqueous solution of formaldehyde 30% (3 mL, 32 mmol). The solution was allowed to stand overnight, saturated with NaCl, and extracted with chloroform (3 × 50 mL). The organic layer was washed with water and dried over $MgSO_4$. The solvent was removed in a vacuum and the residue was purified by column chromatography on silica (Kieselgel 60, Merck, chloroform as eluent) to yield 1 g (74%) of **11**, as a colorless oil (Found: C, 73.55; H, 8.83; N, 10.88. Calcd for $C_{16}H_{24}N_2O$: C, 73.81; H, 9.29; N, 10.76); ν_{max} (KBr)/cm^{-1} 3057, 2974, 2936, 2878, 2809, 1681, 1576, 1540, 1495, 1460, 1444, 1362, 1335, 1264, 1247, 1170, 1142, 1101, 1040, 1022, 996, 948, 843, 814, and 764; λ_{max} (EtOH)/nm 279 (log ϵ 3.70); δ_H (400 MHz; $CDCl_3$) 0.85 (6 H, t, $J = 7$ Hz, 2 × CH_3, Et), 1.44 (6 H, s, $2CH_3$), 1.63 and 2.05 (both 2 H, dq, $J_1 = 14$ Hz, $J_2 = 7$ Hz, $2CH_2$), 2.41 (3 H, s, N−CH_3), 7.40 (3 H, m, Ph-*m*,*p*), and 7.97 (2 H, m, Ph-*o*); δ_C (75 MHz; $CDCl_3$) 8.4 (CH_3, Et), 25.8 (CH_3), 26.0 (N−CH_3), 28.5 (CH_2), 64.5 (C5), 95.00 (C2), 144.5 (C4), Ph: 128.4 (C−*i*), 128.6 (C−*o*), 128.1 (C−*m*), and 129.5 (C−*p*).

2,2-Diethyl-5,5-diphenyl-3,4,4-trimethylimidazolidin-1-oxyl (12). A solution of **11** (1 g, 3.8 mmol) in dry THF (20 mL) was added dropwise to a 1 M solution of PhLi in diethyl ether (10 mL). The reaction mixture was stirred under argon for 1 h, and then quenched with a saturated solution of NH_4Cl in water. The organic layer was separated and water solution was extracted with ether (2 × 20 mL). The combined organic phase was stirred with $MgSO_4$ and MnO_2 (2 g, 23 mmol) for 1 h. The resulting solution was filtered, the solvent was removed in a vacuum, and the residue was separated with column chromatography on Al_2O_3 to yield **12**, 0.77 g (60%), mp 91−93 °C (hexane) (Found: C, 78.18; H, 8.74; N, 8.23. Calcd for $C_{22}H_{29}N_2O$: C, 78.30; H, 8.66; N, 8.30); ν_{max} (KBr)/cm^{-1} 3050, 2977, 2941, 2879, 2812, 1599, 1491, 1466, 1444, 1388, 1330, 1262, 1231, 1144, 984, 924, 764, 747, and 705.

Time Resolved-CIDNP. A sample, purged with argon and sealed in a standard NMR Pyrex ampule, was irradiated by a excimer laser (wavelength 308 nm, pulse energy up to 150 mJ) in the probe of a 200 MHz NMR spectrometer. TR-CIDNP experiments were carried out with the usual pulse sequence: presaturation−laser pulse−evolution time−detection pulse−free induction decay. Because the background signals in CIDNP spectra are suppressed by the presaturation pulses, only signals of the polarized products formed during the variable delay between the laser and NMR radio frequency (rf) pulse appear in the CIDNP spectra. The rf pulse used has a duration of 3 μs, which corresponds to a flip angle of 30°.

Laser Flash Photolysis. A detailed description of our LFP experiments has been published.[42] Solutions in a rectangular cell with inner dimensions 10 mm × 10 mm were irradiated with a excimer 308 nm laser with pulse energy up to 100 mJ and pulse duration of 15−20 ns. The monitoring system includes a xenon short-arc lamp connected to a high current pulser, a homemade monochromator, a photomultiplier, and a digitizer. The monitoring light, concentrated in a rectangular of 3 mm height and 1 mm width, passed through the cell along the front of the laser irradiated window. Thus, in all experiments the excitation optical length was 1 mm, and the monitoring optical length was 8 mm. To obtain one kinetic trace, 15−20 signals were averaged. All solutions were bubbled with argon for 15 min prior to and all the time during the experiments.

Acknowledgment. This work was supported by the University of Provence, CNRS, RFBR (grant Nos. 05-03-32370 and 04-03-32299), CRDF RUC1-2635-NO-05. D.Z. is very grateful to grant INTAS YS N 05-109-5102 and the financial support of the Zamaraev Scientific Foundation. We are thankful to Prof. M. Forbes for useful discussion.

JO060787X

---

(42) Molokov, I. F.; Tsentalovich, Y. P.; Yurkovskaya, A. V.; Sagdeev, R. Z. *J. Photochem. Photobiol. A*: *Chem.* **1997**, *110*, 159.